A CASSCF/CASPT2 and TD-DFT Study of the Low-Lying Excited States of η_5-CpMn(CO)$_3$

Jürgen Full,[†] Leticia González,*[,†] and Chantal Daniel*[,‡]

Institüt für Chemie-Physikalische und Theoretische Chemie, Freie Universität Berlin, Takustrasse 3, D-14195 Berlin, Germany, and Laboratoire de Chimie Quantique, UMR 7551 CNRS/Université Louis Pasteur, Institut Le Bel, 4 Rue Blaise Pascal, 67000 Strasbourg, France

Received: June 7, 2000; In Final Form: October 19, 2000

The electronic and geometric structures of η_5-CpMn(CO)$_3$ in the near-UV region are investigated through CASSCF/CASPT2 and TD-DFT methods. The optimized geometries obtained at different levels of calculation are compared to the crystal and gas-phase structures for the electronic ground state. The change of geometry when going from the electronic ground state to the low-lying excited states was analyzed on the basis of gradient-CASSCF calculations. The lowest excited-state b^1A' corresponding to a $3d_{Mn} \rightarrow 3d_{Mn}$ excitation calculated at 25 733 cm^{-1} (3.22 eV) and the d^1A' calculated at 30 366 cm^{-1} (3.80 eV) with very low oscillator strengths (<0.007) do not show any significant geometry changes with respect to the electronic ground state. The main geometry changes which never exceed 10% correspond to elongations of the Mn−Cp and Mn−CO bonds (with the out-of-plane CO ligands). The c^1A' ($3d_{Mn} \rightarrow 3d_{Mn}$) absorbing state calculated at 26 470 cm^{-1} (3.31 eV) with an oscillator strength of 0.0157 is characterized by an elongation of the Mn−CO$_{ax}$ bond (CO$_{ax}$ being the in-plane carbonyl) and does not converge to a minimum, which is a characteristic of dissociative states. Among the $^1A''$ ($3d_{Mn} \rightarrow 3d_{Mn}$) states calculated between 24 972 and 29 949 cm^{-1} only the lowest one has an oscillator strength exceeding 0.01. The metal to ligand charge transfer (MLCT) states ($3d_{Mn} \rightarrow \pi^*_{CO}$) are calculated between 37 410−45 019 cm^{-1} and are well separated from the metal centered (MC) ($3d_{Mn} \rightarrow 3d_{Mn}$) states (≈1.0 eV). The time-dependent DFT excitation energies and related assignments compare rather well to the multistate-CASPT2 results as far as the lowest MC excited states are concerned.

1. Introduction

The photochemical reactivity of η_5-CpMn(CO)$_3$ (Cp = η_5-C$_5$H$_5$) has been widely used in substitution reactions of CO by different nucleophilic ligands L[1]

$$\eta_5\text{-CpMn(CO)}_3 \xrightarrow[\text{L}]{h\nu} \eta_5\text{-CpMn(CO)}_2\text{L} + \text{CO} \qquad (1)$$

The unsaturated fragment η_5-CpMn(CO)$_2$ has been detected through IR spectra recorded in low-temperature matrices or frozen hydrocarbon glasses[2,3] and more recently as polymer-bound in polyethylene films[4] under supercritical fluids conditions at room temperature using TRIR. The η_5-CpM (CO)$_3$ complexes (with M = Mn, Re) are good precursors of the Si−H bond activation for which a comparative mechanism has been proposed on the basis of femtosecond to ns pump−probe TRIR experiments completed by ab initio calculations.[5,6] It was found that photolysis of the manganese complex results in dicarbonyl fragments in their singlet and triplet electronic states, whereas photolysis of the rhenium complex lead only to the singlet dicarbonyl. The ultrafast dynamics of the ring closure after photolysis of a variety of (η_5-C$_5$H$_4$R)Mn(CO)$_3$ derivatives (with R = COCH$_3$, COCH$_2$SCH$_3$,CO(CH$_2$)$_2$SCH$_3$, COCH$_2$OCH$_3$, (CH$_2$)$_2$CO$_2$CH$_3$ and CH$_2$CO$_2$CH$_3$)[7] have been investigated. Clearly, according to these recent time-resolved experiments, the dynamical effects including solvation are very important at the early stage of the photolysis of η_5-CpMn(CO)$_3$. A detailed knowledge of the structures of η_5-CpMn(CO)$_3$ and η_5-CpMn-(CO)$_2$ in their ground and excited states is the starting point of the investigation of the photodissociation dynamics of the title molecule. As far as the electronic structure is concerned most of the theoretical studies have been limited to the electronic ground state of η_5-CpMn(CO)$_3$.[8−17] The electronic structure has also been investigated by photoelectron spectroscopy.[9,10,18] To the best of our knowledge no excited states calculations have been performed on cyclopentadienyl tricarbonyl transition metal complexes.

The aim of the present study is to determine the transitions to the low-lying singlet states of η_5-CpMn(CO)$_3$ through CASSCF/ MS−CASPT2 calculations and to investigate (at the DFT and Gradient/CASSCF level of theory) the structure of η_5-CpMn(CO)$_3$ in various electronic states as well as the structure of the unsaturated fragment η_5-CpMn(CO)$_2$ which is the key of the photochemically induced reactivity of the title molecule. The recent fascination for the use of DFT methods in the study of excited states[19−21] convinced us to perform systematic TD-DFT calculations in parallel to the costly and fastidious accurate ab initio treatment whenever it is possible in order to discuss the ability of DFT theory to describe excited states properties in transition metal complexes.

2. Computational Details

The molecular structure of η_5-CpMn(CO)$_3$ has been the subject of numerous studies. In solid state, the molecular structure, as predicted by X-ray diffraction[22−24] possess C_1 symmetry, although deviations from D_{5h} and C_{3v} symmetries in the Cp ring and the Mn(CO)$_3$ fragments, respectively, are very small.

Within experimental error it is therefore justified to consider a global C_s symmetry, where the three equivalent carbonyl

[†] Freie Universität Berlin.
[‡] Université Louis Pasteur.

10.1021/jp002042f CCC: $20.00
Published on Web 12/12/2000

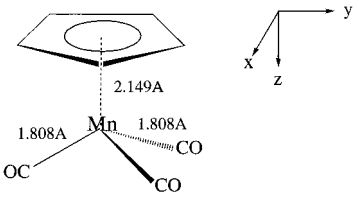

Figure 1. Schematic representation of the staggered conformation of CpMn(CO)$_3$.

groups lie in a staggered configuration with regard to the carbons in the Cp ring (Figure 1).

Gas-phase electron diffraction results[25] at 70 °C are in accord with those obtained by X-ray methods. However, in the gas phase electron diffraction study the precise location of the carbonyl groups with respect to the Cp ring, cannot be detected, suggesting a freely rotating model equally possible, in agreement with extended Hückel calculations which estimate a rotation barrier of 0.0084 kJ/mol for η_5-CpMn(CO)$_3$.[17] For the sake of simplicity, all the calculations described in this paper have been done assuming C_s symmetry and a staggered configuration, as depicted in Figure 1. The geometry optimizations have been performed under C_s symmetry constraint.

Starting from the gas-phase staggered geometry[25] CASSCF optimizations have been performed for the a^1A' electronic ground state and a few low lying singlet A′ excited states in order to follow the geometry change when exciting the molecule. The geometry of η_5- CpMn(CO)$_3$ and η_5- CpMn(CO)$_2$ have been also optimized at the DFT (B3LYP) level. The a^1A' electronic ground-state configuration conforms to a closed shell occupation $(20a')^2$ $(21a')^2$ $(22a')^2$ $(12a'')^2$ $(13a'')^2$ corresponding to the $(3d_{z^2})^2(3_{x^2-y^2})^2(2\pi_{Cp})^2(3d_{xy})^2(1\pi_{Cp})^2$ configuration. Low-lying virtual orbitals correspond to $3d_{yz}$ (23a′), $3d_{xy}$ (14a″) and π^*_{CO} (24a′, 25a′, 15a″ and 16a″).

CASSCF wave functions used in subsequent MS−CASPT2 calculations are averaged over several roots of a given spin and symmetry. Ten electrons are correlated in fourteen orbitals including the highest π_{Cp} occupied orbitals, the $3d_{Mn}$ occupied and vacant orbitals, the 3d of correlation and the low-lying π^*_{CO} orbitals. This active space so-called 10e14a constitutes a good starting point for the addition of dynamical correlation effects by CASPT2 treatment in the multistate approach (with a level shift correction of 0.5). An active space limited to 10 electrons correlated in 10 active orbitals (the previous 10e14a space without the four low-lying π^*_{CO} orbitals) has also been used for the purpose of CASSCF geometry optimizations in order to study the effect of the quality of the CASSCF wave function on the calculated bond lengths and angles. The ground-state CASSCF optimized geometry with the large CASSCF 10e14a active space has been used in the calculation of the Franck−Condon energies and transition dipole moments.

The following basis sets were used in the relativistic effective core potential approximation ECP (small core): a (8s,7p,6d,-1f) set contracted to [6s,5p,3d,1f] ($Z = 15.0$) for the Mn atom,[26] for the oxygen atoms a (4s,5p) set contracted to [2s,3p] ($Z = 6.0$)[27] and for the carbon atoms a (4s,4p) set contracted to [2s,2p] ($Z = 4.0$).[27] The ANO basis set (7s,3p) contracted to [3s,1p] was used for the H atoms.[28] Transition dipole moments were estimated at the CASSCF level.

Vertical excitation energies and transition dipole moments have also been studied using TD-DFT and the same basis set. In particular, two different functionals were used, namely the B3LYP and the local approach BP86. The exchange functional B3 is the hybrid method proposed by Becke[29] that includes a mixture of Slater functional,[30] Becke's 1988 gradient correction[31] and Hartree−Fock exchange. Its correlation part, LYP, is the gradient corrected functional of Lee, Yang and Parr.[32] In the BP86 functional, the exchange-correlation potential corresponds to the gradient approximated potential (GGAs) by Becke[33] for the exchange and Perdew[34] for correlation.

The multiconfigurational calculations have been carried out with the MOLCAS-4 Quantum Chemistry sofware[35] and the TD-DFT with GAUSSIAN-98 series of programs.[36]

3. Results

Structure of η_5-CpMn(CO)$_3$. The CASSCF optimized geometries of η_5-CpMn(CO)$_3$ in its electronic ground state a^1A' and in the three low-lying excited states b^1A', c^1A' and d^1A' corresponding to $3d_{Mn} \rightarrow 3d_{Mn}$ excitations (see next section) are reported in Table 1. The optimized ground-state geometry is compared to the DFT (B3LYP) geometry and to the experimental structures in gas-phase and solid state.

Both CASSCF and DFT optimized bond lengths and bond angles compare rather well to the experimental structures. The agreement between the experimental, the DFT and the gradient-CASSCF optimized structures for the electronic ground state validates our CASSCF active space which has to include the main bonding interactions in our complex. Two different CASSCF active spaces have been used, namely the 10e10a which excludes the four low-lying π^*_{CO} orbitals and the 10e14a adapted to the excited states calculations. The largest deviation which never exceeds 5% is obtained for the Mn−C_{op} distance and the average Mn−C_{ring} distance which are both very sensitive to the CASSCF active space. Indeed, when the π^*_{CO} orbitals are included in the active space the dπ−pπ Mn−CO back-donation is well described (see the Mn−CO bond lengths which agree perfectly with the gas-phase determined values). Consequently, the Mn−Cp interaction (Scheme 2) governed by the $\pi_{Cp}/3d_{Mn}$ stabilizing interaction is significantly affected when going from the CAS10e10a to the CAS10e14a calculation (significant elongation of the calculated Mn−C_{ring} distance).

In any case, this interaction is underestimated both by the DFT method (Mn−C_{ring} = 2.203 Å) and by the CASSCF method (2.231 or 2.215 Å) as compared to the experimental value of 2.149 Å reported in gas phase. On the basis of the results obtained for the a^1A' state, the change of the geometry when going from the electronic ground state to the low-lying singlet excited states b^1A', c^1A' and d^1A' has been investigated through CASSCF calculations. The optimization of the c^1A' state did not converge to a minimum due to the dissociative character of this state. The values reported in Table 1 are the bond lengths and bond angles after 20 cycles of optimization. The main feature is a significant elongation of the Mn−C_{CO} distance of the in-plane carbonyl accompanied by the opening of the bond angle between the two out-of-plane carbonyls. The Mn−Cp and Mn−CO (out-of-plane) bonds are not significantly affected in this excited state. To confirm the dissociative character of the c^1A' state with respect to the in-plane carbonyl loss, potential energy curves will be calculated for this primary reaction. The two other b^1A' and d^1A' excited states converge to optimized structures which are very similar to the electronic ground-state structure. The elongation of the Mn−CO bonds does not exceed 10% in both states and the Mn−Cp bond is not affected when exciting the molecule.

Structure of η_5-CpMn(CO)$_2$. The fragment η_5-CpMn(CO)$_2$ has been optimized at the DFT (B3LYP) level in the singlet closed-shell and triplet electronic configurations. The optimized structures are depicted in Figure 2.

As reported in a previous work,[6] the DFT results show a lower energy for the triplet η_5-CpMn(CO)$_2$ relative to the singlet with

TABLE 1: Optimized CASSCF Geometries of $CpMn(CO)_3$ for the a^1A' Electronic Ground State and the Low-lying b^1A', c^1A' and d^1A' Singlet Excited States

bond length/angle[a]	gas phase[b]	solid state[c]	a^1A' DFT	a^1A' [d]	b^1A'	c^1A' [e]	d^1A'
$Mn-C_{ip}$	1.808	1.780, 1.797	1.793	1.810 (1.830)	1.994 (1.996)	2.846 (2.249)	(1.919) (1.966)
$Mn-C_{op}$	1.808	1.780, 1.797	1.794	1.806 (1.831)	1.977 (1.997)	1.883 (1.904)	(1.960) (1.967)
$Mn-C_{ring}$[f]	2.149	2.124, 2.151	2.203	2.231 (2.215)	2.361 (2.335)	2.245 (2.328)	(2.404) (2.370)
C−O[a]	1.148	1.150, 1.134	1.173	1.148 (1.146)	1.138 (1.138)	1.135 (1.136)	(1.141) (1.139)
C−C[a]	1.424	1.388, 1.394	1.434	1.420 (1.420)	1.418 (1.416)	1.422 (1.415)	(1.421) (1.417)
$C_{ip}-Mn-C_{ip}$	91.9	92.0	94.0	93.2 (93.6)	94.7 (93.4)	85.4 (91.5)	(102.7) (100.4)
$C_{op}-Mn-C_{op}$	91.9	92.0	93.4	92.5 (92.9)	95.0 (93.0)	106.5 (102.2)	(94.0) (91.9)

[a] The bond distances (in Å) and angles (in deg) are compared to the experimental and DFT (B3LYP) data for the electronic ground state (C_{ip} and C_{op} stand for the in-plane and out-of-plane carbon atoms in the $C_s(yz)$ symmetry). [b] Reference 25. [c] Reference 22 and 23, respectively. [d] The values in parentheses are obtained with the 10e10a CASSCF active space. [e] Values after 20 cycles of optimization. [f] Average values.

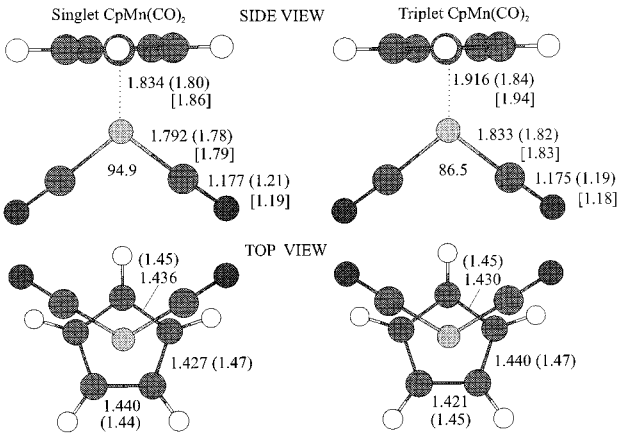

Figure 2. Side and top views of the optimized geometries for the singlet and triplet $CpMn(CO)_2$. Bond distances in angstroms and angles in degrees. Values in parentheses and brackets correspond to MP2/lanl2dz and B3LYP/lanl2dz, respectively, from ref 6.

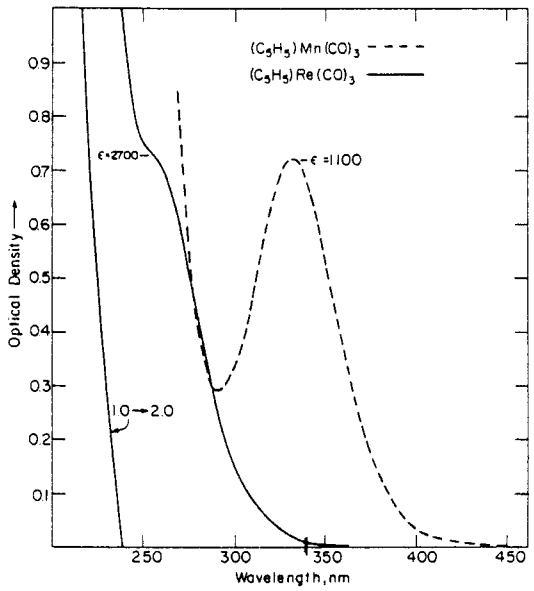

Figure 3. Experimental spectrum from ref 37.

SCHEME 1

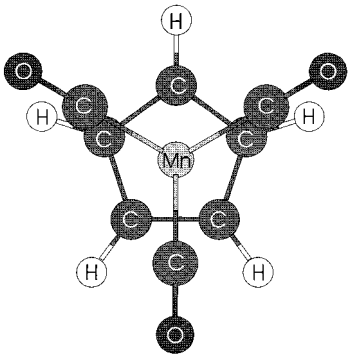

SCHEME 2

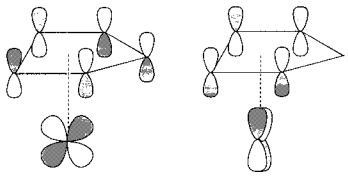

$\Delta E = 5.6$ kcal/mol (vs 8.09 kcal/mol in ref 6). Our results confirm the near-degeneracy of the two electronic configurations in the unsaturated fragment. When going from the reactant $CpMn(CO)_3$ electronic ground state to the low-lying singlet state of $CpMn(CO)_2$ the main deformation is a shortening of the Mn−Cp bond (≈20%) due to the enhancement of the Cp/Mn interaction after the in plane CO loss. This effect is also observed, to a lesser extent in the triplet state which presents an important angular deformation with respect both to the singlet and to the reactant $CpMn(CO)_3$.

Excited States of η_5-$CpMn(CO)_3$. The calculated B3LYP and BP86 excitation energies of the low-lying singlet electronic states of A′ and A″ symmetry and the associated oscillator strengths are reported in Table 2. The lowest part of the absorption spectrum (below 31 000 cm^{-1} or 322 nm) is composed by metal centered transitions corresponding to $3d_{Mn}$ to $3d_{Mn}$ excitations.

This is confirmed by the CASSCF/MS-CASPT2 excitation energies reported in Table 3. The excited states have mixed characters as illustrated by the CI coefficients of the principal configurations which do not exceed 0.5 in most cases. Even though the energetics obtained through the different methods compare rather well, the correlation between the CASSCF and the TD-DFT expansions is difficult to establish and some inconsistency remains at this level as illustrated by the comparison given in Table 4.

At this point it is important to understand that a direct comparison between DFT and CASSCF results is hazardous at molecular orbitals level. Indeed, in the CASSCF/CASPT2 approach the physics is stored in the square of the wave function expanded in term of states configurations. The description of the excited states is obtained by diagonalization in a restricted full-CI scheme limited to the CASSCF active space. In the DFT approach the physics is contained in the density expressed in term of Kohn−Sham orbitals which may significantly differ

TABLE 2: Calculated B3LYP and BP86 Excitation Energies (cm^{-1} and eV) with the Corresponding One-Electron Excitations (Weighting Coefficients in Parentheses) and Oscillator Strengths *f*

B3LYP				BP86			
transition	principal configurations	ΔE	f	transition	principal configuration	ΔE	f
$a^1A' \rightarrow a^1A''$	$3d_{xy} \rightarrow 3d_{yz}$ (−0.43) $3_{x^2-y^2} \rightarrow 3d_{xz}$ (0.48)	25200 (3.15)	0.0000	$a^1A' \rightarrow a^1A''$	$3_{x^2-y^2} \rightarrow 3d_{xz}$ (0.54) $3d_{xy} \rightarrow 3d_{yz}$ (−0.47)	26480 (3.31)	0.0000
$a^1A' \rightarrow b^1A'$	$3d_{xy} \rightarrow 3d_{xz}$ (0.53) $3_{x^2-y^2} \rightarrow 3d_{yz}$ (0.34)	26720 (3.34)	0.0097	$a^1A' \rightarrow b^1A'$	$3d_{xy} \rightarrow 3d_{xz}$ (0.55) $3_{x^2-y^2} \rightarrow 3d_{yz}$ (0.39)	27760 (3.47)	0.0114
$a^1A' \rightarrow b^1A''$	$3d_{z^2} \rightarrow 3d_{xz}$ (0.47) $3d_{xy} \rightarrow 3d_{yz}$ (0.31) $3_{x^2-y^2} \rightarrow 3d_{xz}$ (0.27)	27040 (3.38)	0.0018	$a^1A' \rightarrow b^1A''$	$3d_{xy} \rightarrow 3d_{yz}$ (0.42) $3d_{z^2} \rightarrow 3d_{xz}$ (0.38) $3_{x^2-y^2} \rightarrow 3d_{xz}$ (0.35)	28800 (3.60)	0.0032
$a^1A' \rightarrow c^1A'$	$3d_{z^2} \rightarrow 3d_{yz}$ (0.42) $3_{x^2-y^2} \rightarrow 3d_{yz}$ (−0.42)	27240 (3.41)	0.0025	$a^1A' \rightarrow c^1A'$	$3_{x^2-y^2} \rightarrow 3d_{yz}$ (0.48) $3d_{z^2} \rightarrow 3d_{yz}$ (−0.32) $3d_{xy} \rightarrow 3d_{xz}$ (−0.32)	28880 (3.61)	0.0035
$a^1A' \rightarrow c^1A''$	$3d_{z^2} \rightarrow 3d_{xz}$ (0.45) $3d_{xy} \rightarrow 3d_{yz}$ (−0.31) $3_{x^2-y^2} \rightarrow 3d_{xz}$ (−0.29)	30720 (3.84)	0.0000	$a^1A' \rightarrow c^1A''$	$3d_{z^2} \rightarrow 3d_{xz}$ (0.55) $3d_{xy} \rightarrow 3d_{yz}$ (−0.25) $3_{x^2-y^2} \rightarrow 3d_{xz}$ (−0.23)	30400 (3.80)	0.0000
$a^1A' \rightarrow d^1A'$	$3d_{z^2} \rightarrow 3d_{yz}$ (0.48) $3_{x^2-y^2} \rightarrow 3d_{yz}$ (0.29) $3d_{xy} \rightarrow 3d_{xz}$ (−0.26)	30960 (3.87)	0.0000	$a^1A' \rightarrow d^1A'$	$3d_{z^2} \rightarrow 3d_{yz}$ (0.59) $3_{x^2-y^2} \rightarrow 3d_{yz}$ (0.22) $3d_{xy} \rightarrow 3d_{xz}$ (−0.18)	30720 (3.84)	0.0001
$a^1A' \rightarrow d^1A''$	$3d_{xy} \rightarrow \pi^*_{CO}$(0.67)	33200 (4.15)	0.0005	$a^1A' \rightarrow d^1A''$	$3d_{xy} \rightarrow \pi^*_{CO}$(0.67)	34240 (4.28)	0.0004
$a^1A' \rightarrow e^1A'$	$3_{x^2-y^2} \rightarrow \pi^*_{CO}$(0.66)	33200 (4.15)	0.0000	$a^1A' \rightarrow e^1A'$	$3_{x^2-y^2} \rightarrow \pi^*_{CO}$(0.67)	34240 (4.28)	0.0005
$a^1A' \rightarrow e^1A''$	$3d_{xy} \rightarrow \pi^*_{CO}$(0.52) $3_{x^2-y^2} \rightarrow \pi^*_{CO}$(−0.37)	36240 (4.53)	0.0003	$a^1A' \rightarrow e^1A''$	$3d_{xy} \rightarrow \pi^*_{CO}$(0.59) $3_{x^2-y^2} \rightarrow \pi^*_{CO}$(−0.39)	37200 (4.65)	0.0002
$a^1A' \rightarrow f^1A''$	$3_{x^2-y^2} \rightarrow \pi^*_{CO}$(0.54) $3d_{xy} \rightarrow \pi^*_{CO}$(0.38)	36800 (4.60)	0.0113	$a^1A' \rightarrow f^1A'$	$3_{x^2-y^2} \rightarrow \pi^*_{CO}$(0.45) $3d_{xy} \rightarrow \pi^*_{CO}$(−0.37)	37440 (4.68)	0.0014
$a^1A' \rightarrow f^1A'$	$3d_{xy} \rightarrow \pi^*_{CO}$(0.46) $3_{x^2-y^2} \rightarrow \pi^*_{CO}$(−0.47)	36800 (4.60)	0.0132	$a^1A' \rightarrow f^1A''$	$3_{x^2-y^2} \rightarrow \pi^*_{CO}$(0.51) $3d_{xy} \rightarrow \pi^*_{CO}$(0.29) $3d_{xy} \rightarrow \pi^*_{CO}$(0.27)	37600 (4.70)	0.0024
$a^1A' \rightarrow g^1A'$	$3d_{z^2} \rightarrow \pi^*_{CO}$(0.57) $3d_{xy} \rightarrow \pi^*_{CO}$(−0.26) $3_{x^2-y^2} \rightarrow \pi^*_{CO}$(−0.25)	39840 (4.98)	0.0207	$a^1A' \rightarrow g^1A'$	$3_{x^2-y^2} \rightarrow \pi^*_{CO}$(0.40) $3_{x^2-y^2} \rightarrow \pi^*_{CO}$(−0.33) $3_{x^2-y^2} \rightarrow \pi^*_{CO}$(0.31) $3d_{z^2} \rightarrow \pi^*_{CO}$(0.25)	37680 (4.71)	0.0011

TABLE 3: Calculated CASSCF and MS-CASPT2 Excitation Energies (cm^{-1} and eV) with the Corresponding One-Electron Excitations (Weighting Coefficients Given in Parentheses), Weight Coefficient of the Reference CASSCF Function ω and CASSCF Oscillator Strengths *f*

transition	principal configurations	CASSCF	MS−CASPT2	w	f
a^1A'				0.733	
$a^1A' \rightarrow a^1A''$	$3d_{z^2} \rightarrow 3d_{xz}$ (0.42) $3d_{xy} \rightarrow 3d_{yz}$ (0.44)	32021 (3.97)	24972 (3.10)	0.723	0.0110
$a^1A' \rightarrow b^1A'$	$3d_{xy} \rightarrow 3d_{xz}$ (−0.51) $3d_{x^2-y^2} \rightarrow 3d_{yz}$ (0.46)	34678 (4.33)	25733 (3.22)	0.721	0.0069
$a^1A' \rightarrow b^1A''$	$3d_{x^2-y^2} \rightarrow 3d_{xz}$ (0.68)	30779 (3.82)	26024 (3.23)	0.726	0.0085
$a^1A' \rightarrow c^1A'$	$3d_{z^2} \rightarrow 3d_{yz}$ (∼0.9)	32488 (4.06)	26470 (3.30)	0.724	0.0157
$a^1A' \rightarrow c^1A''$	$3_{x^2-y^2}/3_{dz^2} \rightarrow 3d_{xz}$ (0.55) $3d_{xy} \rightarrow 3d_{yz}$ (−0.37)	37882 (4.70)	29949 (3.71)	0.720	0.0002
$a^1A' \rightarrow d^1A'$	$3d_{x^2-y^2}/3_{dz^2} \rightarrow 3d_{yz}$ (0.56) $3d_{xy} \rightarrow 3d_{xz}$ (0.42)	38396 (4.80)	30366 (3.80)	0.722	0.0015
$a^1A' \rightarrow e^1A'$	$3d_{x^2-y^2} \rightarrow \pi^*_{CO}$ (−0.57) $3_{dz^2}/3_{dx^2-y^2} \rightarrow \pi^*_{CO}$ (0.41)	41149 (5.14)	36075 (4.51)	0.724	0.0000
$a^1A' \rightarrow d^1A''$	$3d_{xy} \rightarrow \pi^*_{CO}$ (−0.74)	40249 (4.99)	37410 (4.63)	0.727	0.0001
$a^1A' \rightarrow f^1A'$	$3d_{xy} \rightarrow \pi^*_{CO}$ (0.63) $3d_{z^2} \rightarrow \pi^*_{CO}$ (0.42)	47733 (5.91)	40690 (5.09)	0.720	0.0040
$a^1A' \rightarrow g^1A'$	$3d_{xy} \rightarrow \pi^*_{CO}$ (0.72) $3d_{z^2} \rightarrow \pi^*_{CO}$ (−0.21)	46629 (5.80)	41175 (5.15)	0.723	0.0052
$a^1A' \rightarrow e^1A''$	$3d_{x^2-y^2} \rightarrow \pi^*_{CO}$ (0.83) $3d_{z^2} \rightarrow \pi^*_{CO}$ (0.21)	43278 (5.37)	42346 (5.25)	0.730	0.0000
$a^1A' \rightarrow f^1A''$	$3d_{z^2} \rightarrow \pi^*_{CO}$ (−0.82)	47939 (5.94)	45019 (5.58)	0.727	0.0004

from the CASSCF molecular orbitals. The description of the excited states is obtained by single excitations in the space described by the Kohn−Sham orbitals.

The $a^1A' \rightarrow b^1A'$, $a^1A' \rightarrow c^1A'$ and $a^1A' \rightarrow d^1A'$ transitions corresponding to $3d_{Mn} \rightarrow 3d_{Mn}$ excitations and calculated at 25 733, 26 470, and 30 366 cm^{-1}, respectively, at the MS-CASPT2 level and at 26 720 cm^{-1} (27 760 cm^{-1}), 27 240 cm^{-1} (28 880 cm^{-1}), and 30 960 cm^{-1} (30 720 cm^{-1}), respectively, at the DFT level (values obtained with the BP86 functional are given in parentheses) contribute to the first shoulder of the absorption spectrum starting at 26 666 cm^{-1} (375 nm) with a maximum at 30 769 cm^{-1} (325 nm) (Figure 3).[37] To a lesser extent, the $a^1A' \rightarrow a^1A''$, the $a^1A' \rightarrow b^1A''$ and the $a^1A' \rightarrow c^1A''$ transitions corresponding to $3d_{Mn} \rightarrow 3d_{Mn}$ excitations and calculated between 24 972 and 29 949 cm^{-1} at the CASPT2 level and between 25 200 and 30 720 cm^{-1} at the DFT level (B3LYP) should also contribute to this first band. The four low-lying singlet states of CpMn(CO)$_3$ are nearly degenerate and should contribute to the main UV absorption of this molecule according to the qualitative oscillator strengths reported in Tables 2 and 3. The experimental spectrum shows a second band with a rather high intensity at 36 360 cm^{-1} (275 nm) with a peak around 250 nm (40 000 cm^{-1}) (Figure 3) assigned to the $a^1A' \rightarrow f^1A'$ and $a^1A' \rightarrow g^1A'$ transitions corresponding to

TABLE 4: Low-Lying $^1A'$ Excited States of $CpMn(CO)_3$ Calculated at the CASSCF/MS-CASPT2 and TD-DFT Levels of Theory

	b^1A'			c^1A'			d^1A'		
	CASPT2	B3LYP	BP86	CASPT2	B3LYP	BP86	CASPT2	B3LYP	BP86
excitation energies (cm^{-1})	25 733	26 720	27 760	26 470	27 240	28 880	30 366	30 960	30 720
oscillator strengths	0.0069	0.0097	0.0114	0.0157	0.0025	0.0035	0.0015	0.0	0.0001
$3d_{xy} \rightarrow 3d_{xz}$	−0.51	0.53	0.55			−0.32	0.42	−0.26	−0.18
$3d_{x^2-y^2} \rightarrow 3d_{yz}$	0.46	0.34	0.39		−0.42	0.48	0.28	0.29	0.22
$3d_{z^2} \rightarrow 3d_{yz}$				0.90	0.42	−0.32	0.28	0.48	0.59
	e^1A'			f^1A'			g^1A'		
	CASPT2	B3LYP	BP86	CASPT2	B3LYP	BP86	CASPT2	B3LYP	BP86
excitation energies (cm^{-1})	36 075	33 200	34 240	41 175	36 800	37 440	40 690	39 840	37 680
oscillator strengths	0.0	0.0	0.0005	0.0052	0.0132	0.0014	0.004	0.0207	0.0011
$3d_{xy} \rightarrow \pi^*_{CO}$				0.72	0.46	−0.37	0.63	−0.26	
$3d_{x^2-y^2} \rightarrow \pi^*_{CO}$	−0.57	0.66	0.67		−0.47	0.45		−0.25	0.40
$3d_{z^2} \rightarrow \pi^*_{CO}$	0.41			−0.21			0.42	0.57	0.25

$3d_{Mn} \rightarrow \pi^*_{CO}$ excitations and calculated at 40 690 and 41 175 cm^{-1}, respectively at the MS−CASPT2 level. The $a^1A' \rightarrow e^1A'$ (36 075 cm^{-1}), $a^1A' \rightarrow d^1A''$ (37 410 cm^{-1}), $a^1A' \rightarrow e^1A''$ (42 346 cm^{-1}), and $a^1A' \rightarrow f^1A''$ (45 019 cm^{-1}) have very low oscillator strengths and should contribute to a lesser extent to this second band. The TD-DFT excitation energies of the $^1A'$ ($3d_{Mn} \rightarrow \pi^*_{CO}$) excited states are calculated at 33 200 cm^{-1} (34 240 cm^{-1}), 36 800 cm^{-1} (37 600 cm^{-1}), and 39 840 cm^{-1} (37 680 cm^{-1}) and differ from the MS-CASPT2 values by more than 2000 cm^{-1}. In a recent paper [19] some general trends have been extracted from a comparative study performed on the electronic spectra of a number of unsaturated organic molecules. In particular the difficulty in describing charge transfer states in a dipeptide model has been attributed to insufficient flexibility in the functionals to describe states with extensive charge separations. More generally it seems that the TD-DFT method has some difficulties at describing correctly the highest part of the absorption spectrum where a number of states mixing and near-degeneracy situations may occur.

4. Conclusion

A careful analysis, based on CASSCCF/CASPT2 and TD-DFT calculations, of the lowest part of the electronic spectrum of $MnCp(CO)_3$ has been reported. The first band has been assigned to the $a^1A' \rightarrow {}^1A'$ and $a^1A' \rightarrow {}^1A''$ transitions calculated between 25 000 and 31 000 cm^{-1} (CASPT2 or TD-DFT level of theory) and corresponding to $3d_{Mn} \rightarrow 3d_{Mn}$ excitations. This band is well separated of the second one attributed to metal-to-ligand charge transfer (MLCT) excited states corresponding to $3d_{Mn} \rightarrow \pi^*_{CO}$ excitations calculated between 36 075 and 45 019 cm^{-1} at the CASPT2 level. While the CASSCF/CASPT2 and TD-DFT results exhibit a rather good agreement as far as the low-lying excited states are concerned the position of the second series of excited states seems to be underestimated by the TD-DFT calculations which indicate an energy range between 33 000 cm^{-1} and 39 000 cm^{-1}. This effect could be due to a drawback of the functional which is well adapted to the description of metal centered excited states but which is less good for describing delocalized situations such as in MLCT excited states.

According to the present calculations, the MLCT states corresponding to $3d_{Mn} \rightarrow \pi^*_{Cp}$ excitations are rejected in the upper energy domain of the absorption spectrum of $MnCp(CO)_3$ and do not contribute either to the visible or UV spectrum (below 45 000 cm^{-1} or 220 nm).

To follow the photodissociation mechanism of this molecule under UV irradiation, the potential energy curves associated with the absorbing low-lying singlet states have been calculated. Preliminary wave packet propagations indicate a total and fast CO loss (<100 fs) in agreement with ultrafast laser experiments.[38]

Acknowledgment. The authors are grateful to Roland Lindh for providing a preliminar version of the MS-CASPT2 software. We thank the Deutsche Forschungemeinschaft SFB 450 "Analysis and control of ultrafast photoinduced reactions". The QC calculations have been performed on the HP workstations of the Theoretische Chemie group, Freie Universität Berlin.

References and Notes

(1) Wrighton, M. S. *Chem. Rev.* **1974**, *74*, 401.
(2) Rest, A. J.; Sodeau, J. R.; Taylor, D. J. *J. Chem. Soc., Dalton Trans* **1978**, 651.
(3) Black, J. D.; Boylan, M. J.; Braterman, P. S. *J. Chem. Soc., Dalton Trans* **1981**, 673.
(4) Clarke, M. J.; Howdle, S. M.; Jobling, M.; Poliakoff, M. *J. Am. Chem. Soc.* **1994**, *116*, 8621.
(5) Yang, H.; Kotz, K. T.; Asplund, M. C.; Harris, C. B. *J. Am. Chem. Soc.* **1997**, *119*, 9564.
(6) Yang, H.; Asplund, M. C.; Kotz, K. T.; Wilkers, M. J.; Frei, H.; Harris, C. G. *J. Am. Chem. Soc.* **1998**, *120*, 10154.
(7) Jiao, T.; Pang, Z.; Burkey, T. S.; Johnson, R. F.; Heiner, T. A.; Kleiman, V. D.; Heilweill, E. J. *J. Am. Chem. Soc.* **1999**, *121*, 4618.
(8) Orgel, L. E. *J. Inorg. Nucl. Chem.* **1957**, *2*, 315.
(9) Whitesides, T. H.; Lichtenberger, D. L.; Budnik, R. A. *Inorg. Chem.* **1975**, *141*, 68.
(10) Lichtenberger, D. L.; Fenske, R. F. *J. Am. Chem. Soc.* **1976**, *98*, 50.
(11) Byers, B. P.; Hall, M. B. *Organometallics* **1987**, *6*, 2319.
(12) Böhm, M. C. J. *J. Mol. Struct. THEOCHEM* **1983**, *9*, 73.
(13) Böhm, M. C. *J. Chem. Phys.* **1983**, *78*, 7044.
(14) Brown, C. A.; Fitzpatrick, N. J.; Mathews, N. J. *J. Organomet. Chem.* **1975**, *88*, C27.
(15) Fitzpatrick, N. J.; Savariault, J.; Labarre, J. R. *J. Organomet. Chem.* **1977**, *127*, 325.
(16) Modelli, A.; Distefano, G.; Guerra, M.; Jones, D. *J. Am. Chem. Soc.* **1987**, *109*, 4440.
(17) Albright, T. A.; Hofmann, P.; Hoffmann, R. *J. Am. Chem. Soc.* **1977**, *99*, 7546.
(18) Field, B. N.; Green, J. C.; Moody, A. G. J.; Siegel, M. R. F. *Chem. Phys. Lett.* **1996**, *206*, 211.
(19) Tozer, D. J.; Amos, R. D.; Handy, N. C.; Roos, B. O.; Serrano-Andres, L. *Mol. Phys.* **1999**, *97*, 859.
(20) van Gisbergen, S. J. A.; Groeneveld, J. A.; Rosa, A.; Snijders, J. G.; Baerends, E. J. *J. Phys. Chem. A* **1999**, *103*, 6835.
(21) Rosa, A.; Baerends, E. J.; van Gisbergen, S. J. A.; van Lenthe, E.; Groeneveld, J. A.; Snijders, J. G. *J. Am. Chem. Soc.* **1999**, *121*, 10356.
(22) Berndt, A. F.; Marsh, R. E. *Acta Crystallogr.* **1963**, *16*, 118.
(23) Fitzpatrick, P. J.; Le Page, Y.; Sedman, J.; Butler, I. S. *Inorg. Chem.* **1981**, *20*, 2853.

(24) Cowie, J.; Hamilton, E. J.; Laurie, J. C. V.; Welch, A. J. *J. Organomet. Chem*. **1990**, *394*, 1.
(25) Almond, M. J.; Page, E. M.; Rice, D. A.; Hagen, K.; Vidar Volden, H. *J. Mol. Struct*. **1994**, *319*, 223.
(26) Dolg, M.; Wedig, U.; Stoll, H.; Preuss, H. *J. Chem. Phys*. **1987**, *86*, 866.
(27) Bergner, A.; Dolg, M.; Kuechle, W.; Stoll, H.; Preuss, H. *Mol. Phys.* **1993**, *80*, 1431.
(28) Pierloot, K.; Dumez, B.; Windmark, P. O.; Roos, B. O. *Theor. Chim. Acta* **1995**, *90*, 87.
(29) Becke, A. D. *J. Chem. Phys.* **1993**, *98*, 5648.
(30) Slater, J. C. *Quantum Theory of Molecules and Solids*; MacGraw-Hill: New York, 1974; Vol. 4.
(31) Becke, A. D. *J. Chem. Phys.* **1988**, *88*, 1053.
(32) Lee, W. Y.; Parr, R. G. *Phys. Rev.* **1988**, *B37*, 785.
(33) Becke, A. D. *Phys. Rev.* **1988**, *A38*, 3098.
(34) Perdew, J. P. *Phys. Rev.* **1986**, *B33*, 8822.
(35) Andersson, K.; Blomberg, M. R. A.; Fülscher, M. P.; Karlström, G.; Lindh, R.; Malmqvist, P.-Å.; Neagrady, P.; Olsen, J.; Roos, B. O.; Sadlej, A. J.; Schütz, M.; Seijo, L.; Serrano-Andrés, L.; Siegbahn, P. E. M.; Widmark, P.-O. MOLCAS 4.1; University of Lund: Sweden, 1998.
(36) Frisch, M. J.; Trucks, G. W.; Schlegel, H. B.; Scuseria, G. E.; Robb, M. A.; Cheeseman, J. R.; Zakrzewski, V. G.; Montgomery, J. A., Jr.; Stratmann, R. E.; Burant, J. C.; Dapprich, S.; Millam, J. M.; Daniels, A. D.; Kudin, K. N.; Strain, M. C.; Farkas, O.; Tomasi, J.; Barone, V.; Cossi, M.; Cammi, R.; Mennucci, B.; Pomelli, C.; Adamo, C.; Clifford, S.; Ochterski, J.; Petersson, G. A.; Ayala, P. Y.; Cui, Q.; Morokuma, K.; Malick, D. K.; Rabuck, A. D.; Raghavachari, K.; Foresman, J. B.; Cioslowski, J.; Ortiz, J. V.; Baboul, A. G.; Stefanov, B. B.; Liu, G.; Liashenko, A.; Piskorz, P.; Komaromi, I.; Gomperts, R.; Martin, R. L.; Fox, D. J.; Keith, T.; Al-Laham, M. A.; Peng, C. Y.; Nanayakkara, A.; Gonzalez, C.; Challacombe, M.; Gill, P. M. W.; Johnson, B.; Chen, W.; Wong, M. W.; Andres, J. L.; Gonzalez, C.; Head-Gordon, M.; Replogle, E. S.; Pople, J. A. *Gaussian98*, Revision A.7; Gaussian, Inc., Pittsburgh, PA, 1998.
(37) Giordano, P. J.; Wrighton, M. S. *Inorg. Chem*. **1977**, *16*, 160.
(38) Bartelt, A.; Daniel, C.; Full, J.; González, L.; Kreuz, M.; Lupulescu, C.; Manz, J.; Oppel, M.; Rosendo-Francisco, P.; Vajda, S.; Woste, L. *Chem. Phys*., submitted.